Theta vacuum effects on QCD phase diagram

Sakai, Yuji
Department of Physics, Graduate School of Sciences, Kyushu University

Kouno, Hiroaki
Department of Physics, Saga University

Sasaki, Takahiro
Department of Physics, Graduate School of Sciences, Kyushu University

Yahiro, Masanobu
Department of Physics, Graduate School of Sciences, Kyushu University

https://hdl.handle.net/2324/25619

Theta vacuum effects on QCD phase diagram

Yuji Sakai,[1, *] Hiroaki Kouno,[2, †] Takahiro Sasaki,[1, ‡] and Masanobu Yahiro[1, §]

¹Department of Physics, Graduate School of Sciences,

Kyushu University, Fukuoka 812-8581, Japan

²Department of Physics, Saga University, Saga 840-8502, Japan

(Dated: November 9, 2011)

Abstract

Theta vacuum effects on the QCD phase structure in the μ-T plane are studied by using the Polyakov-loop extended Nambu-Jona-Lasinio model and its extension, where μ is the quark chemical potential and T is temperature, respectively. As the parameter θ of the theta vacuum increases, the chiral transition becomes stronger. For large θ, it eventually becomes first order even at zero μ.

———
[*] sakai@phys.kyushu-u.ac.jp

[†] kounoh@cc.saga-u.ac.jp

[‡] sasaki@phys.kyushu-u.ac.jp

[§] yahiro@phys.kyushu-u.ac.jp

I. INTRODUCTION

Violations of parity (P), charge conjugation (C) and charge-parity symmetries (CP) are important subjects in particle and nuclear physics. For example, the strong CP problem is a long-standing puzzle; see for example Ref. [1] for a review of this problem. Lorentz and gauge invariance allow the Quantum Chromodynamics (QCD) action to have a term

$$\mathcal{L}_\theta = \theta \frac{g^2}{64\pi^2} \epsilon^{\mu\nu\sigma\rho} F^a_{\mu\nu} F^a_{\sigma\rho} \tag{1}$$

of the topological charge, where $F^a_{\mu\nu}$ is the field strength of gluon. The parameter θ can take any arbitrary value between $-\pi$ and π, where $\theta = -\pi$ is identical with $\theta = \pi$. Nevertheless, experiment indicates $|\theta| < 3 \times 10^{-10}$ [2, 3]. Since θ is P-odd (CP-odd), P (CP) is then preserved for $\theta = 0$ and $\pm\pi$, but explicitly broken for other θ. Why is θ so small ? This is the so-called strong CP problem.

For zero temperature (T) and zero quark-chemical potential (μ), P is conserved at $\theta = 0$, as Vafa and Witten showed [4]. Meanwhile, P is spontaneously broken at $\theta = \pi$, as Dashen [5] and Witten [6] pointed out. This is the so-called Dashen phenomena. Since the spontaneous P violation is a nonperturbative phenomenon, the phenomenon was so far studied mainly with the effective model such as the chiral perturbation theory [7–12], the Nambu-Jona-Lasinio (NJL) model [13–15] and the Polyakov-loop extended Nambu-Jona-Lasinio (PNJL) model [16].

For T higher than the QCD scale Λ_{QCD}, there is a possibility that a finite θ, depending on spacetime coordinates (t, x), is effectively induced, since sphalerons are so activated as to jump over the potential barrier between the different degenerate ground states [17]. If so, P and CP symmetries can be violated locally in high-energy heavy-ion collisions or the early universe at $T \approx \Lambda_{\mathrm{QCD}}$. Actually, it is argued in Refs. [12, 18] that θ may be of order one during the QCD phase transition in the early universe, while it vanishes at the present epoch [19–23]. This finite θ may be a new source of very large CP violation in the Universe and may be a crucial missing element for solving the puzzle of baryogenesis.

Furthermore, this effective $\theta(t, x)$ deviates the total number of particles plus antiparticles with right-handed helicity from that with left-handed helicity. The magnetic field, formed in the early stage of heavy-ion collision, will lift the degeneracy in spin depending on the charge of particle. As a consequence of this fact, an electromagnetic current is generated along the magnetic field, since particles with right-handed helicity move opposite to antiparticles with right-handed helicity.

2

This is the so-called chiral magnetic effect (CME) [18, 24–26]. CME may explain the charge separations observed in the recent STAR results [27]. Thus, the thermal system with nonzero θ is quite interesting.

In this letter, we study effects of the theta-vacuum on QCD phase diagram by using the two-flavor PNJL model [16, 28–44] and its extension; see Ref. [16] and references therein for further information on the PNJL model. Particularly, our attention is focused on the two-flavor phase diagram in the μ-T plane, where μ is the quark chemical potential. In our previous work Ref. [16], as a theoretical interest, we investigated spontaneous P and C violations at finite θ and imaginary μ. As physical phenomena that may occur in the early universe or the high-energy heavy-ion collisions, we here examine the chiral and P symmetry restorations at finite T and θ and real μ.

This paper is organized as follows. In section II, the PNJL model and its extension are explained briefly. In section III, the numerical results are shown. Section IV is devoted to summary.

II. PNJL MODEL

Pioneering work on the parity violation and its restoration in the framework of the NJL model [13–15, 45–47] was done by Fujihara, Inagaki and Kimura [13]. Boer and Boomsma studied this issue extensively [14, 15]. In Ref. [16], we have extended their formalism based on the NJL model to that on the PNJL model. The two-flavor ($N_f = 2$) PNJL Lagrangian with the θ-dependent anomaly term is

$$
\begin{aligned}
\mathcal{L} = {} & \bar{q}(i\gamma_\nu D^\nu - m)q - \mathcal{U}(\Phi[A], \Phi[A]^*, T) \\
& + G_1 \sum_{a=0}^{3} \left[(\bar{q}\tau_a q)^2 + (\bar{q}i\gamma_5\tau_a q)^2 \right] + 8G_2 \left[e^{i\theta} \det(\bar{q}_R q_L) + e^{-i\theta} \det(\bar{q}_L q_R) \right],
\end{aligned} \tag{2}
$$

where $q = (u, d)$ denotes the two-flavor quark field, m does the current quark-mass matrix $\mathrm{diag}(m_u, m_d)$, τ_0 is the 2×2 unit matrix, $\tau_a (a = 1, 2, 3)$ are the Pauli matrices and $D^\nu = \partial^\nu + iA^\nu - i\mu\delta_0^\nu$. The field A^ν is defined as $A^\nu = \delta_0^\nu g A_a^0 \frac{\lambda^a}{2}$ with the gauge field A_a^ν, the Gell-Mann matrix λ_a and the gauge coupling g. In the NJL sector, G_1 denotes the coupling constant of the scalar and pseudoscalar-type four-quark interaction, and G_2 is the coupling constant of the Kobayashi-Maskawa-'t Hooft determinant interaction [48, 49] the matrix indices of which run in the flavor space. The Polyakov potential $\mathcal{U}$, defined later in (19), is a function of the

3

Polyakov loop Φ and its Hermitian conjugate Φ^*,

$$\Phi = \frac{1}{N_{\mathrm{c}}} \mathrm{Tr} L, \quad \Phi^* = \frac{1}{N_{\mathrm{c}}} \mathrm{Tr} L^\dagger \tag{3}$$

with

$$L(\mathbf{x}) = \mathcal{P} \exp\left[i \int_0^\beta d\tau A_4(\mathbf{x}, \tau) \right], \tag{4}$$

where $\mathcal{P}$ is the path ordering and $A_4 = iA_0$. In the chiral limit ($m_{\mathrm{u}} = m_{\mathrm{d}} = 0$), the Lagrangian density has the exact $SU(N_f)_{\mathrm{L}} \times SU(N_f)_{\mathrm{R}} \times U(1)_{\mathrm{v}} \times SU(3)_{\mathrm{c}}$ symmetry. The $U(1)_{\mathrm{A}}$ symmetry is explicitly broken if $G_2 \neq 0$. The temporal component of the gauge field is diagonal in the flavor space, because the color and the flavor spaces are completely separated out in the present case. In the Polyakov gauge, L can be written in a diagonal form in the color space [29]:

$$L = e^{i\beta(\phi_3 \lambda_3 + \phi_8 \lambda_8)} = \mathrm{diag}(e^{i\beta\phi_a}, e^{i\beta\phi_b}, e^{i\beta\phi_c}), \tag{5}$$

where $\phi_a = \phi_3 + \phi_8/\sqrt{3}$, $\phi_b = -\phi_3 + \phi_8/\sqrt{3}$ and $\phi_c = -(\phi_a + \phi_b) = -2\phi_8/\sqrt{3}$. The Polyakov loop Φ is an exact order parameter of the spontaneous $\mathbb{Z}_3$ symmetry breaking in the pure gauge theory. Although the $\mathbb{Z}_3$ symmetry is not an exact one in the system with dynamical quarks, it may be a good indicator of the deconfinement phase transition. Therefore, we use Φ to define the deconfinement phase transition. For simplicity, we assume below that $m_{\mathrm{u}} = m_{\mathrm{d}} = m_0$.

We transform the quark field q to the new one q' with

$$q_R = e^{i\frac{\theta}{4}} q'_R, \quad q_L = e^{-i\frac{\theta}{4}} q'_L, \tag{6}$$

in order to remove the θ dependence of the determinant interaction. Under this $\mathrm{U}(1)_{\mathrm{A}}$ transformation, the quark-antiquark condensates are also transformed as

$$
\begin{aligned}
\sigma &\equiv \bar{q}q = \cos\left(\frac{\theta}{2}\right)\sigma' + \sin\left(\frac{\theta}{2}\right)\eta', \\
\eta &\equiv \bar{q}i\gamma_5 q = -\sin\left(\frac{\theta}{2}\right)\sigma' + \cos\left(\frac{\theta}{2}\right)\eta', \\
a_i &\equiv \bar{q}\tau_i q = \cos\left(\frac{\theta}{2}\right)a'_i + \sin\left(\frac{\theta}{2}\right)\pi'_i, \\
\pi_i &\equiv \bar{q}i\tau_i\gamma_5 q = -\sin\left(\frac{\theta}{2}\right)a'_i + \cos\left(\frac{\theta}{2}\right)\pi'_i,
\end{aligned}
\tag{7}
$$

where σ' is defined by the same form as σ but q is replaced by q'; this is the case also for other

condensates η', a_i' and π_i'. The Lagrangian density is then rewritten with q' as

$$
\begin{aligned}
\mathcal{L} &= \bar{q}'(i\gamma_\nu D^\nu - m_{0+} - im_{0-}\gamma_5)q' - \mathcal{U}(\Phi[A], \Phi[A]^*, T) \\
&+ G_1 \sum_{a=0}^{3} \left[(\bar{q}'\tau_a q')^2 + (\bar{q}'i\gamma_5\tau_a q')^2\right] \\
&+ 8G_2 \left[\det(\bar{q}'_R q'_L) + \det(\bar{q}'_L q'_R)\right],
\end{aligned}
\tag{8}
$$

where $m_{0+} = m_0 \cos\left(\frac{\theta}{2}\right)$ and $m_{0-} = m_0 \sin\left(\frac{\theta}{2}\right)$. Making the mean field approximation and performing the path integral over the quark field, one can obtain the thermodynamic potential Ω (per volume) for finite T and μ:

$$
\begin{aligned}
\Omega = -2 \int \frac{d^3\mathrm{p}}{(2\pi)^3} &\Big[3\{E_+(\mathrm{p}) + E_-(\mathrm{p})\} + \frac{1}{\beta} \ln\left[1 + 3\Phi e^{-\beta E_+^-} + 3\Phi^* e^{-2\beta E_+^-} + e^{-3\beta E_+^-}\right] \\
&+ \frac{1}{\beta} \ln\left[1 + 3\Phi e^{-\beta E_-^-} + 3\Phi^* e^{-2\beta E_-^-} + e^{-3\beta E_-^-}\right] + \frac{1}{\beta} \ln\left[1 + 3\Phi^* e^{-\beta E_+^+} + 3\Phi e^{-2\beta E_+^+} + e^{-3\beta E_+^+}\right] \\
&+ \frac{1}{\beta} \ln\left[1 + 3\Phi^* e^{-\beta E_-^+} + 3\Phi e^{-2\beta E_-^+} + e^{-3\beta E_-^+}\right] + U + \mathcal{U},
\end{aligned}
\tag{9}
$$

where $E_+^\pm = E_+(\mathbf{p}) \pm \mu$ and $E_-^\pm = E_-(\mathbf{p}) \pm \mu$ with

$$
\begin{aligned}
E_\pm &= \sqrt{\mathbf{p}^2 + C \pm 2\sqrt{D}}, \tag{10} \\
C &= M^2 + N^2 + A^2 + P^2, \tag{11} \\
D &= A^2 M^2 + P^2 N^2 + 2APMN\cos\varphi + A^2 P^2 \sin^2\varphi \\
&= (M\mathbf{A} + N\mathbf{P})^2 + (\mathbf{A} \times \mathbf{P})^2 \geq 0 \tag{12} \\
M &= m_{0+} - 2G_+\sigma' = m_{0+} - 2(G_1 + G_2)\sigma', \tag{13} \\
N &= m_{0-} - 2G_-\eta' = m_{0-} - 2(G_1 - G_2)\eta', \tag{14} \\
\mathbf{A} &= (-2G_- a_1', -2G_- a_2', -2G_- a_3'), \tag{15} \\
\mathbf{P} &= (-2G_+ \pi_1', -2G_+ \pi_2', -2G_+ \pi_3'), \tag{16} \\
A &= \sqrt{\mathbf{A} \cdot \mathbf{A}}, \quad P = \sqrt{\mathbf{P} \cdot \mathbf{P}}, \quad \mathbf{A} \cdot \mathbf{P} = AP\cos\varphi, \tag{17} \\
U &= G_+(\sigma'^2 + \pi_a'^2) + G_-(a_a'^2 + \eta'^2). \tag{18}
\end{aligned}
$$

In the right-hand side of (9), only the first term diverges. The term is then regularized by the three-dimensional momentum cutoff Λ [29, 30]. Following Ref. [14, 15], we introduce c as $G_1 = (1-c)G$ and $G_2 = cG$, where $0 \leq c \leq 0.5$ and $G > 0$. Hence, the NJL sector has four parameters of m_0, Λ, G and c. We put $m_0 = 5.5\mathrm{MeV}$. The parameters Λ and G are so chosen as to reproduce the pion decay constant $f_\pi = 93\mathrm{MeV}$ and the pion mass $m_\pi = 139\mathrm{MeV}$ at vacuum. The remaining

5

parameter c is a free parameter. Although the exact value of c is unknown, it is known from the analysis of the η-η' splitting in the three-flavor model that $c \sim 0.2$ is favorable [50]. The value $c = 0.2$ has been also used in Refs. [14, 15]. Therefore, we take $c = 0.2$ also here.

The PNJL model is reduced to the NJL model in the limit of $T = 0$, since in (9) the Polyakov-loop potential $\mathcal{U}$ tends to zero and the logarithmic terms approach $N_c \Theta(\mu - E_\pm^\pm)$, where $\Theta(x) = 1$ for $x > 0$ and $\Theta(x) = 0$ for $x < 0$, in the limit. Since P breaking at $T = 0$ and $\theta = \pi$ has already been studied in detail by the NJL model [13–15], we here concentrate ourselves on P restoration at finite T and $\theta = \pi$.

The Polyakov potential $\mathcal{U}$ of Ref. [31] is fitted to LQCD data in the pure gauge theory at finite T [51, 52]:

$$\mathcal{U} = T^4 \Big[-\frac{a(T)}{2} \Phi^* \Phi + b(T) \ln(1 - 6\Phi^* \Phi + 4(\Phi^3 + \Phi^{*3}) - 3(\Phi \Phi^*)^2) \Big], \qquad (19)$$

$$a(T) = a_0 + a_1 \Big(\frac{T_0}{T}\Big) + a_2 \Big(\frac{T_0}{T}\Big)^2, \quad b(T) = b_3 \Big(\frac{T_0}{T}\Big)^3. \qquad (20)$$

The parameters included in $\mathcal{U}$ are summarized in Table I. The Polyakov potential yields a first-order deconfinement phase transition at $T = T_0$ in the pure gauge theory. The original value of T_0 is 270 MeV evaluated by the pure gauge lattice QCD calculation. However, the PNJL model with this value of T_0 yields a larger value of the transition temperature at zero chemical potential than the full LQCD simulation [53–56] predicts. Therefore, we rescale T_0 to 212 MeV [36] so that the PNJL model can reproduce the critical temperature 173 MeV of the full LQCD simulation.

a_0	a_1	a_2	b_3
3.51	-2.47	15.2	-1.75

TABLE I: Summary of the parameter set in the Polyakov-potential sector used in Ref. [31]. All parameters are dimensionless.

The variables $X = \Phi, \Phi^*, \sigma, \pi_i, \eta$ and a_i satisfy the stationary conditions,

$$\partial \Omega / \partial X = 0. \qquad (21)$$

The solutions of the stationary conditions do not give the global minimum Ω necessarily. There is a possibility that they yield a local minimum or even a maximum. We then have checked that the solutions yield the global minimum when the solutions $X(T, \theta, \mu)$ are inserted into (9). For $\theta = 0$ and π, the thermodynamic potential Ω is invariant under P transformation,

$$\eta \to -\eta, \quad \pi_a \to -\pi_a. \qquad (22)$$

Since the four-quark coupling constant G contains effects of gluons, G may depend on Φ. In fact, recent calculations [57–59] of the exact renormalization group equation (ERGE) [60] suggest that the higher-order mixing interaction is induced by ERGE. It is highly expected that the functional form and the strength of the entanglement vertex $G(\Phi)$ are determined in future by these theoretical approaches. In Ref. [42], we assumed the following form

$$G(\Phi) = G[1 - \alpha_1 \Phi\Phi^* - \alpha_2(\Phi^3 + \Phi^{*3})] \tag{23}$$

by respecting the chiral symmetry, P symmetry, C symmetry [16, 38] and the extended $\mathbb{Z}_3$ symmetry. This model is called the entanglement PNJL (EPNJL) model. The EPNJL model with the parameter set [42], $\alpha_1 = \alpha_2 = 0.2$ and $T_0 = 190$ MeV, can reproduce LQCD data at imaginary chemical potential [61–70] and real isospin chemical potential [71] as well as the results at zero chemical potential [53–55]. Recently, it was shown in Ref. [43] that, also under the strong magnetic field, the EPNJL model yields results consistent with the LQCD data [72]. The EPNJL model with this parameter set is also applied to the present case with real μ and finite θ.

III. NUMERICAL RESULTS

The present PNJL model has eight condensates of quark-antiquark pair. However, $\vec{a}$ and $\vec{\pi}$ vanish [14–16], since $m_{\mathrm{u}} = m_{\mathrm{d}}$ and the isospin chemical potential is not considered here. We can then concentrate ourselves on σ, η and Φ. We can also restrict θ in a period $0 \leq \theta \leq 2\pi$ without loss of generality.

Figure 1 shows T dependence of σ and Φ at $\mu = 0$ and $\theta = 0$; note that $\eta = 0$ in this case. In both the PNJL and EPNJL models, σ (Φ) rapidly but continuously decreases (increases) as T increases. Therefore, the chiral restoration and the deconfinement transition are crossover. The crossover transitions occur more rapidly in the EPNJL model than in the PNJL model.

Figure 2 presents T dependence of σ, η and Φ at $\mu = 0$ and $\theta = \pi$; note that this figure plots condensates σ and η before the transformation (6). For both the PNJL and EPNJL models, the eta condensation ($\eta \neq 0$) occurs at low T and hence P symmetry is spontaneously broken there. At high T, in contrast, $\eta = 0$ and hence P symmetry is restored. The critical temperature T_P of P restoration is 202 (170) MeV in the PNJL (EPNJL) model.

The order of P restoration was reported to be of second order in the NJL model [14, 15] but of first order in the linear sigma model [73]. In the EPNJL (PNJL) model, η is discontinuous
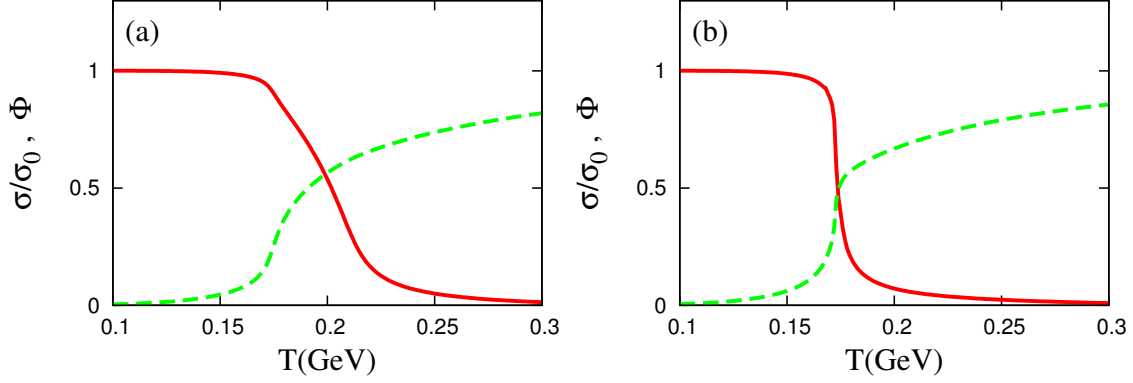
7

Fig. 1: T dependence of the chiral condensate σ (solid line) and the Polyakov loop Φ (dashed line) at $\mu = 0$ and $\theta = 0$. Panel (a) represents results with PNJL model, while panel (b) does results of the EPNJL model. The chiral condensate is normalized by the value σ_0 at $T = \theta = 0$.

in its zeroth (first) order. Thus, the PNJL model supports the second-order transition, but the EPNJL model does the first-order. The zeroth-order discontinuity (gap) of η in the EPNJL model is propagated to other quantities σ and Φ as the zeroth-order discontinuity (gap), according to the discontinuity theorem by Barducci, Casalbuoni, Pettini and Gatto [74]. This really takes place in Fig. 2, although the discontinuity (gap) is appreciable for Φ but very tiny for σ. The first-order discontinuity (cusp) of η in the PNJL model is also propagated to σ and Φ as the first-order discontinuity (cusp) [37]. As mentioned above, the EPNJL model is more consistent with the LQCD data than the PNJL model. This means that the order of P restoration may be weak first order.

T dependence of σ, η and Φ is shown also for $\mu = 300$MeV and $\theta = \pi$ in Fig. 3. In the case of large μ, P restoration is of first order in both the PNJL and EPNJL models. As μ increase with θ fixed at π, thus, P restoration changes from the second order to the first order in the PNJL model, while it is always of first-order in the EPNJL model. This means that there is a tricritical point (TCP) in the PNJL model; note that the TCP is a point where the first- and second-order transitions meet each other.

Figure 4 shows the phase diagram of P restoration in the μ-T plane for the case of $\theta = \pi$. In the PNJL model of panel (a), point A at $(\mu, T) = (209\,[\text{MeV}], 165\,[\text{MeV}])$ is a TCP of P restoration, while there is no TCP in the EPNJL model of panel (b).

Figure 5 represents the phase diagram of the chiral transition in the μ-θ-T space. These dia-
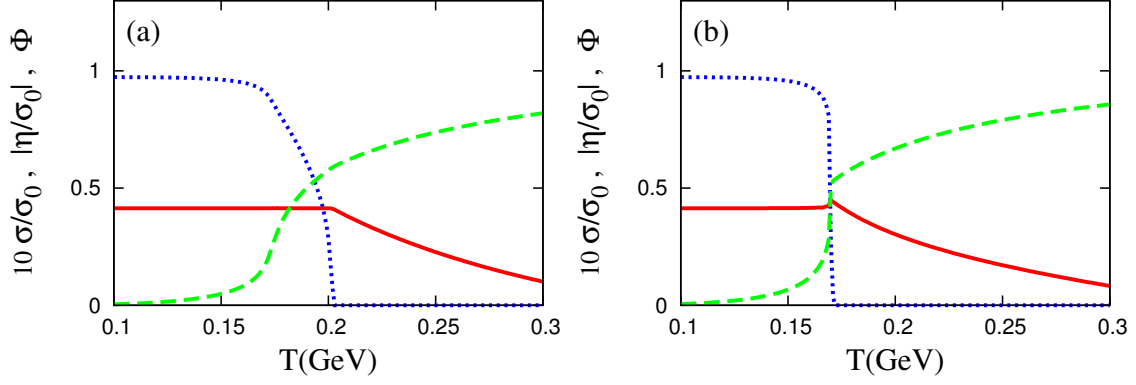
Fig. 2: T dependence of the chiral condensate σ (solid line), the eta condensate η (dotted line) and the Polyakov loop Φ (dashed line) at $\mu = 0$ and $\theta = \pi$. Panel(a) stands for results of the PNJL model, while panel (b) does results of the EPNJL model.
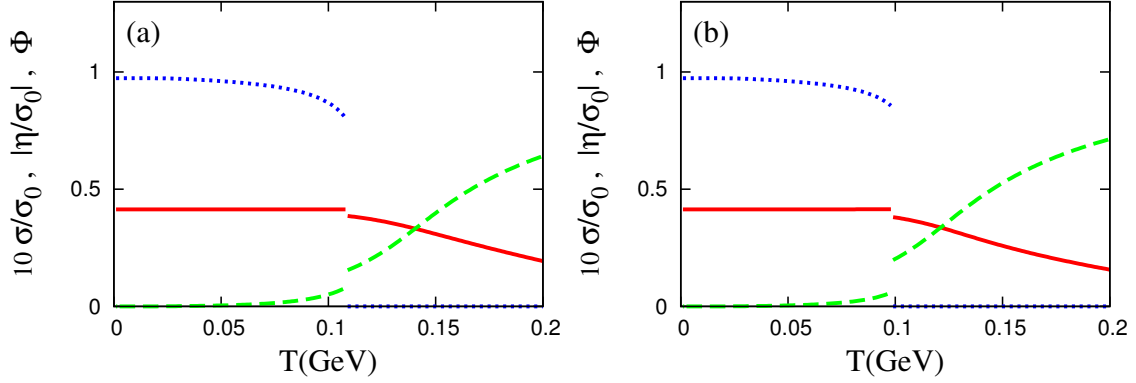

Fig. 3: T dependence of the chiral condensate σ (solid line), the eta condensate η (dotted line) and the Polyakov loop Φ (dashed line) at $\mu = 300\text{MeV}$ and $\theta = \pi$. Panel(a) stands for results of the PNJL model, while panel (b) does results of the EPNJL model.

grams are mirror symmetric with respect to the μ-T plane at $\theta = \pi$. At finite θ, $\sqrt{\sigma^2 + \eta^2}$ is the order parameter of the chiral transition rather than σ itself [16]. In the PNJL model of panel (a), point A in the μ-T plane at $\theta = \pi$ is a TCP of P restoration and a critical endpoint (CEP) of chiral restoration at which the first-order (solid) line is connected to the crossover (dotted) line. Point C in the μ-T plane at $\theta = 0$ is another CEP of the chiral transition [46, 75]. The second-order (dashed) line from C to A is a trajectory of CEP with respect to increasing θ from 0 to π. Thus, the CEP (point C) at $\theta = 0$ is a remnant of the TCP (point A) of P restoration at $\theta = \pi$. In the EPNJL
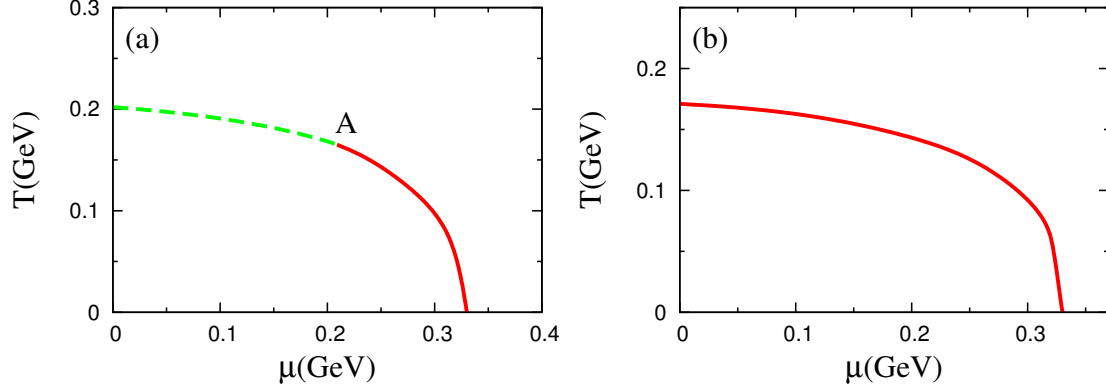
Fig. 4: Phase diagram of P restoration at $\theta = \pi$. Panel(a) stands for results of the PNJL model, while panel (b) does results of the EPNJL model. The solid and dashed lines represent the P restoration of first-order and second-order, respectively. Point A in panel (a) is a TCP

model of panel (b), no TCP and then no CEP appears in the μ-T plane at $\theta = \pi$. The second-order (dashed) line starting from point C never reaches the μ-T plane at $\theta = \pi$. For both the PNJL and EPNJL models, the location of CEP in the μ-T plane moves to higher T and lower μ as θ increases from 0 to π. Particularly in the EPNJL model, the chiral transition is always first order in the μ-T plane at $\theta = \pi$.
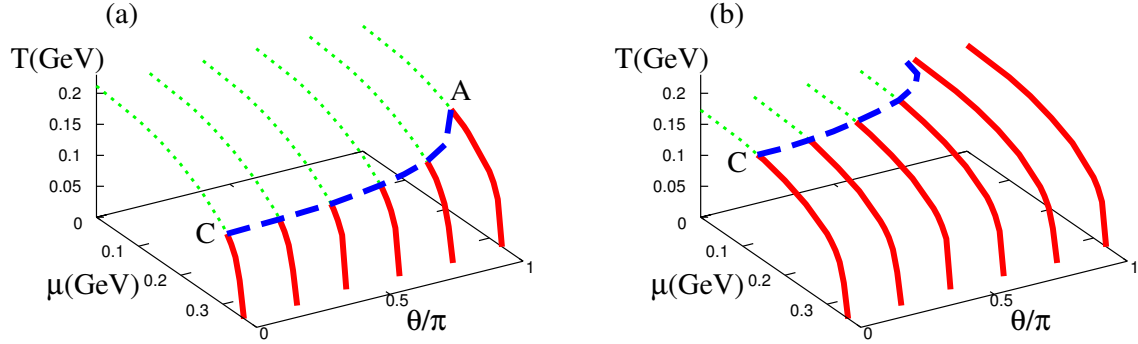

Fig. 5: Phase diagram of the chiral restoration in the $\mu - \theta - T$ space. The solid, dashed and dotted lines represent the chiral transitions of first-order, second-order and crossover, respectively. Point A is a CEP of chiral restoration and a TCP of P restoration, while point C is a CEP of chiral restoration. Panel(a) stands for results of the PNJL model, while panel (b) does results of the EPNJL model.

Figure 6 shows the projection of the second-order chiral-transition line in the μ-θ-T space on

10

the μ-θ plane. The solid (dashed) line stands for the projected line in the EPNJL (PNJL) model. The first-order transition region exists on the right-hand side of the line, while the left-hand side corresponds to the chiral crossover region. The first-order transition region is much wider in the EPNJL model than in the PNJL model. In the EPNJL model, eventually, the chiral transition becomes first order even at $\mu = 0$ when θ is large.
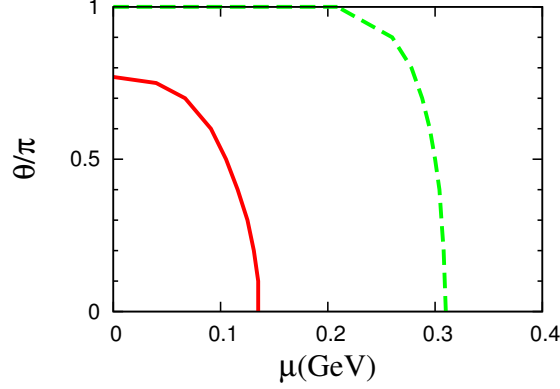

Fig. 6: Projection of the second-order chiral-transition line in the μ-θ-T space on the μ-θ plane. The solid (dashed) line corresponds to the line in the EPNJL (PNJL) model.

QCD has the anomalous Ward identities among the chiral and eta condensates, σ and η, the gluon condensate $\langle \frac{g^2}{64\pi^2} \epsilon^{\alpha\beta\sigma\rho} F^a_{\mu\nu} F^a_{\sigma\rho} \rangle$ and the topological susceptibility χ_t [12]:

$$\frac{\partial \Omega}{\partial \theta} = \langle \frac{g^2}{64\pi^2} \epsilon^{\alpha\beta\sigma\rho} F^a_{\mu\nu} F^a_{\sigma\rho} \rangle = \frac{1}{N_f} m_0 \eta, \tag{24}$$

$$\frac{\partial^2 \Omega}{\partial \theta^2} = -\chi_t = -\frac{1}{N_f^2} m_0 \sigma + \mathcal{O}(m_0^2). \tag{25}$$

The identities are useful for checking the self-consistency of the proposed model [12]. The gluon condensate does not appear explicitly in the PNJL model, but the model satisfies

$$\frac{\partial \Omega}{\partial \theta} = \frac{1}{N_f} m_0 \eta. \tag{26}$$

The PNJL model also satisfies the second Ward identity (25) as shown below. In the PNJL model, the left-hand side of (25) is rewritten into

$$\frac{\partial^2 \Omega}{\partial \theta^2} = \left(\frac{\partial^2 \Omega}{\partial \theta^2} \right)_{\text{fixed } \phi_i} - \sum_{i,j} \frac{\partial^2 \Omega}{\partial \theta \partial \phi_i} \left(\frac{\partial^2 \Omega}{\partial \phi_i \partial \phi_j} \right)^{-1} \frac{\partial^2 \Omega}{\partial \theta \partial \phi_j} \tag{27}$$

with the inverse curvature matrix

$$C_{ij}^{-1} = \left(\frac{\partial^2 \Omega}{\partial \phi_i \partial \phi_j} \right)^{-1} \tag{28}$$

11

for the parameters $\phi = (\sigma', \eta', \Phi, \Phi^*)$. Note that C_{ij}^{-1} is the susceptibility χ_{ij} of order parameters ϕ_i and ϕ_j and the term including χ_{ij} is of order $O(m_0^2)$. Equation (27) turns out to be the second Ward identity (25) after simple algebraic calculations. For $\theta = 0$, Eq. (27) is further rewritten into

$$\frac{\partial^2 \Omega}{\partial \theta^2} = -\frac{1}{4} m_0 \sigma + \frac{1}{4} \frac{\Omega_{NN}^0}{(2G_- \Omega_{NN}^0 + 1)} m_0^2, \tag{29}$$

in the virtue of the θ-reflection symmetry, where $\Omega_{NN}^0 = \frac{\partial^2 \Omega^0}{\partial N^2}$ for the thermodynamic potential Ω^0 with no the meson potential U and no the Polyakov potential $\mathcal{U}$.
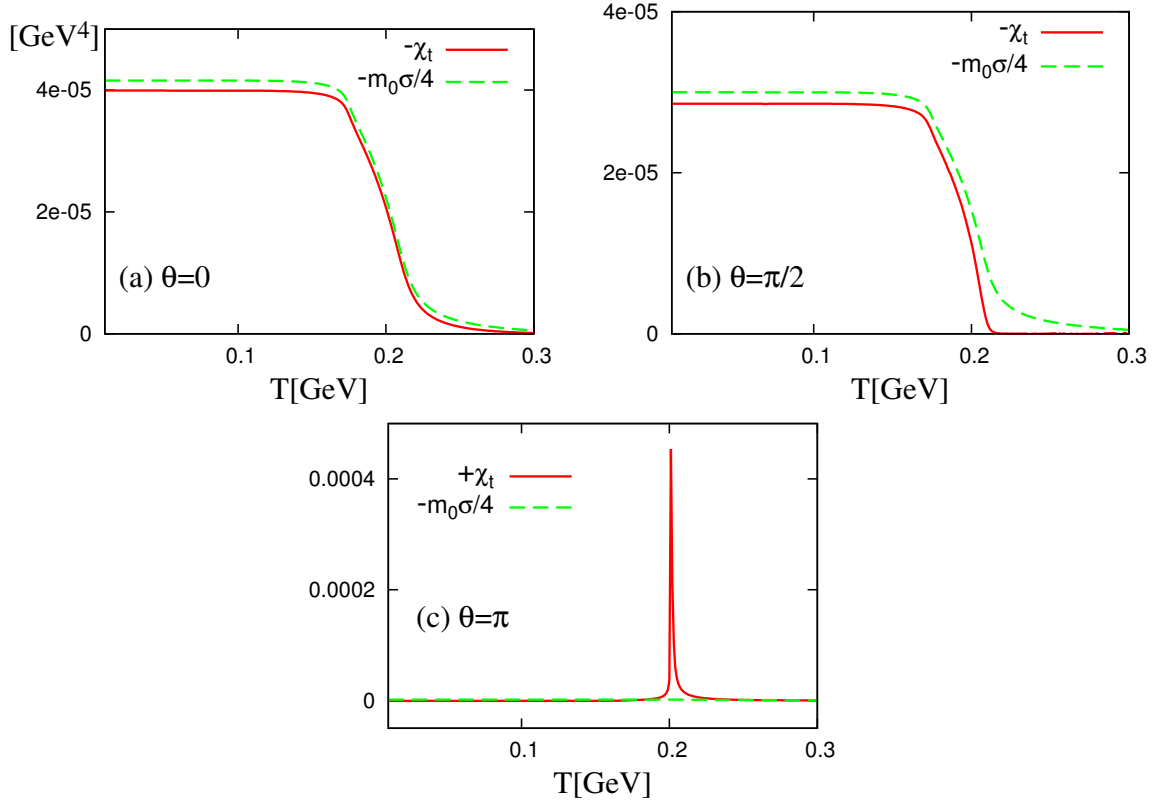
Fig. 7: T dependence of the topological susceptibility χ_t (solid line) and the chiral condensate σ (dashed line) at (a) $\theta = 0$, (b) $\pi/2$, and (c) π. These are results of the PNJL model at $\mu = 0$.

Figure 7 shows the topological susceptibility χ_t and the quantity $m_0 \sigma / 4$ as a function of T at $\theta = 0$, $\pi/2$ and π, where the case of $\mu = 0$ is considered. As shown in panels (a) and (b), the topological susceptibility almost agrees with $m_0 \sigma / 4$ for $\theta \leq \pi/2$. The small deviation between the two quantities shows that the corrections of order $O(m_0^2)$ to the approximate identity $\chi_t = \frac{1}{N_f^2} m_0 \sigma$ are small. In panel (c) for $\theta = \pi$, the both quantities are still close to each other except for the critical temperature $T \approx 200$ MeV of the second-order P transition. Near the critical temperature,

12

the susceptibility χ_{ij} of the order parameters becomes large and hence the corrections of order $O(m_0^2)$ coming from the second term of the right-hand side of (27) become significant.

IV. SUMMARY

In summary, we have investigated theta-vacuum effects on QCD phase diagram, using the PNJL and EPNJL models. For the both models, the chiral transition becomes strong as θ increases. Particularly in the EPNJL model that is more reliable than the PNJL model, it becomes first order even at $\mu = 0$ when θ is large. This is an important result. If the chiral transition becomes first order at zero μ, it will change the scenario of cosmological evolution. For example, the first-order transition allows us to think the inhomogeneous Big-Bang nucleosynthesis model or a new scenario of baryogenesis. Our analyses are based on the two-flavor PNJL (EPNJL) model and effects of the strange quark are then neglected. It is very interesting to study the effects by using the three-flavor PNJL model [40].

[1] E. Vicari and H. Panagopoulos, Phys. Rept. **470**, 93 (2009).

[2] C. A. Baker, et al., Phys. Rev. Lett. **97**, 131801 (2006).

[3] K. Kawarabayashi and N. Ohta, Nucl. Phys. **B175**, 477 (1980); Prog. Theor. Phys. **66**, 1789 (1981); N. Ohta, Prog. Theor. Phys. **66**, 1408 (1981); [Erratum-ibid. **67** (1982) 993].

[4] C. Vafa and E. Witten, Phys. Rev. Lett. **53**, 535 (1984).

[5] R. Dashen, Phys. Rev. D **3**, 1879 (1971).

[6] E. Witten, Ann. Phys. **128**, 363 (1980).

[7] P. di Vecchia, and G. Veneziano, Nucl. Phys. **B171**, 253 (1980).

[8] A. V. Smilga, Phys. Rev. D **59**, 114021 (1999).

[9] M. H. G. Tytgat, Phys. Rev. D **61**, 114009 (2000).

[10] G. Akemann, J. T. Lenaghan, and, K. Splittorff, Phys. Rev. D **65**, 085015 (2002).

[11] M. Creutz, Phys. Rev. Lett. **92**, 201601 (2004).

[12] M. A. Metlitski, and A. R. Zhitnitsky, Nucl. Phys. **B731**, 309 (2005); Phys. Lett. B **633**, 721 (2006).

[13] T. Fujihara, T. Inagaki, and D. Kimura, Prog. Theor. Phys. **117**, 139 (2007).

[14] D. Boer and J. K. Boomsma, Phys. Rev. D **78**, 054027 (2008).

[15] J. K. Boomsma and D. Boer, Phys. Rev. D **80**, 034019 (2009).

[16] H. Kouno, Y. Sakai, T. Sasaki, K. Kashiwa, and M. Yahiro, Phys. Rev. D **83**, 076009 (2011).

[17] L. McLerran, E. Mottola and M. E. Shaposhnikov, Phys. Rev. D **43**, 2027 (1991).

[18] D. Kharzeev, and A. Zhitnitsky, Nucl. Phys. A **797**, 67 (2007).

[19] R. D. Peccei and H. R. Quinn, Phys. Rev. D **16**, 1791 (1977).

[20] J. W. Kim, Phys. Rev. Lett. **43**, 103 (1979).

[21] M. A. Shifman A. I. Vainstein and V. I. Zakharov, Nucl. Phys. B **166**, 493 (1980).

[22] A. R. Zhitnitsky, Sov. J. Nucl. Phys. **31**, 260 (1980).

[23] M. Dine W. Fischler and M. Srednicki, Phys. Lett. B **104**, 199 (1981).

[24] D. Kharzeev, Phys. Lett. B **633**, 260 (2006); D. Kharzeev, L. D. McLerran, and H. J. Warringa, Nucl. Phys. A **803**, 227 (2008).

[25] K. Fukushima, D. E. Kharzeev, and H. J. Warringa, Phys. Rev. D **78**, 074033 (2008).

[26] K. Fukushima, M. Ruggieri, and R. Gatto, Phys. Rev. D **81**, 114031 (2010).

[27] B. I. Abelev et al. [STAR Collaboration], Phys. Rev. Lett. **103**, 251601 (2009); Phys. Rev. C **81**, 054908 (2010).

[28] P. N. Meisinger, and M. C. Ogilvie, Phys. Lett. B **379**, 163 (1996).

[29] K. Fukushima, Phys. Lett. B **591**, 277 (2004); Phys. Rev. D **77**, 114028 (2008).

[30] C. Ratti, M. A. Thaler, and W. Weise, Phys. Rev. D **73**, 014019 (2006); C. Ratti, S. Rößner, M. A. Thaler, and W. Weise, Eur. Phys. J. C **49**, 213 (2007).

[31] S. Rößner, C. Ratti, and W. Weise, Phys. Rev. D **75**, 034007 (2007).

[32] B. -J. Schaefer, J. M. Pawlowski, and J. Wambach, Phys. Rev. D **76**, 074023 (2007).

[33] K. Kashiwa, H. Kouno, M. Matsuzaki, and M. Yahiro, Phys. Lett. B **662**, 26 (2008).

[34] Y. Sakai, K. Kashiwa, H. Kouno, and M. Yahiro, Phys. Rev. D **77**, 051901(R) (2008); Phys. Rev. D **78**, 036001 (2008).

[35] Y. Sakai, K. Kashiwa, H. Kouno, M. Matsuzaki, and M. Yahiro, Phys. Rev. D **78**, 076007 (2008).

[36] Y. Sakai, K. Kashiwa, H. Kouno, M. Matsuzaki, and M. Yahiro, Phys. Rev. D **79**, 096001 (2009).

[37] K. Kashiwa, M. Yahiro, H. Kouno, M. Matsuzaki, and Y. Sakai, J. Phys. G: Nucl. Part. Phys. **36**, 105001 (2009).

[38] H. Kouno, Y. Sakai, K. Kashiwa, and M. Yahiro, J. Phys. G: Nucl. Part. Phys. **36**, 115010 (2009).

[39] Y. Sakai, H. Kouno, and M. Yahiro, J. Phys. G: Nucl. Part. Phys. **37**, 105007 (2010).

[40] T. Matsumoto, K. Kashiwa, H. Kouno, K. Oda, and M. Yahiro, Phys. Lett. B **694**, 367 (2011).

[41] T. Sasaki, Y. Sakai, H. Kouno and M. Yahiro, Phys. Rev. D **82**, 116004 (2010).

[42] Y. Sakai, T. Sasaki, H. Kouno and M. Yahiro, Phys. Rev. D **82**, 076003 (2010).

[43] R. Gatto and M. Ruggieri, Phys. Rev. D **83**, 034016 (2011).

[44] Y. Sakai, T. Sasaki, H. Kouno, and M. Yahiro, arXiv:arXiv:1104.2394 [hep-ph] (2011).

[45] Y. Nambu and G. Jona-Lasinio, Phys. Rev. **122**, 345 (1961); Phys. Rev. **124**, 246 (1961).

[46] M. Asakawa and K. Yazaki, Nucl. Phys. **A504**, 668 (1989).

[47] K. Kashiwa, H. Kouno, T. Sakaguchi, M. Matsuzaki, and M. Yahiro, Phys. Lett. B **647**, 446 (2007); K. Kashiwa, M. Matsuzaki, H. Kouno, and M. Yahiro, Phys. Lett. B **657**, 143 (2007).

[48] M. Kobayashi, and T. Maskawa, Prog. Theor. Phys. **44**, 1422 (1970); M. Kobayashi, H. Kondo, and T. Maskawa, Prog. Theor. Phys. **45**, 1955 (1971).

[49] G. 't Hooft, Phys. Rev. Lett. **37**, 8 (1976); Phys. Rev. D **14**, 3432 (1976); **18**, 2199(E) (1978).

[50] M. Frank, M. Buballa, and M. Oertel, Phys. Lett. B **562**, 221 (2003).

[51] G. Boyd, J. Engels, F. Karsch, E. Laermann, C. Legeland, M. Lütgemeier, and B. Petersson, Nucl. Phys. **B469**, 419 (1996).

[52] O. Kaczmarek, F. Karsch, P. Petreczky, and F. Zantow, Phys. Lett. B **543**, 41 (2002).

[53] F. Karsch, Lect. notes Phys. **583**, 209 (2002).

[54] F. Karsch, E. Laermann, and A. Peikert, Nucl. Phys. B **605**, 579 (2001).

[55] M. Kaczmarek and F. Zantow, Phys. Rev. D **71**, 114510 (2005).

[56] S. Borsányi, et al., JHEP **09**, (2010) 073; JHEP **11**, (2010) 077.

[57] J. Braun, L. M. Haas, F. Marhauser, and J. M. Pawlowski, Phys. Rev. Lett. **106**, 022002 (2011); J. Braun, and A Janot, arXiv:1102.4841[hep-ph] (2011).

[58] K.-I. Kondo, Phys. Rev. D **82**, 065024 (2010).

[59] T. K. Herbst, and J. M. Pawlowski, and B. -J. Schaefer, Phys. Lett. B **696**, 58 (2011).

[60] C. Wetterich, Phys. Lett. B **301**, 90 (1993).

[61] P. de Forcrand and O. Philipsen, Nucl. Phys. B **642**, 290 (2002); **673**, 170 (2003).

[62] M. D'Elia and M. P. Lombardo, Phys. Rev. D **67**, 014505 (2003); **70**, 074509 (2004); M. D'Elia,

F. D. Renzo, and M. P. Lombardo, Phys. Rev. D **76**, 114509 (2007);

[63] H. S. Chen and X. Q. Luo, Phys. Rev. **D72**, 034504 (2005); arXiv:hep-lat/0702025 (2007).

[64] L. K. Wu, X. Q. Luo, and H. S. Chen, Phys. Rev. **D76**, 034505 (2007).

[65] M. D'Elia and F. Sanfilippo, Phys. Rev. D **80**, 014502 (2009).

[66] P. Cea, L. Cosmai, M. D'Elia, C. Manneschi and A. Papa, Phys. Rev. D **80**, 034501 (2009).

[67] M. D'Elia and F. Sanfilippo, Phys. Rev. D **80**, 111501 (2009); C. Bonati, G. Cossu, M. D'Elia and F. Sanfilippo, Phys. Rev. D **83**, 054505 (2011).

[68] P. de Forcrand and O. Philipsen, Phys. Rev. Lett. **105**, 152001 (2010).

[69] K. Nagata, A. Nakamura, Y. Nakagawa, S. Motoki, T. Saito and M. Hamada, Proc. Sci. LAT2009 (2009) 191, arXiv:0911.4164 [hep-lat]; K. Nagata and A. Nakamura, arXiv:1104.2142 [hep-lat]], (2011).

[70] T. Takaishi, P. de Forcrand and A. Nakamura, Proc. Sci. LAT2009 (2009) 198, arXiv:1002.0890 [hep-lat]

[71] J. B. Kogut, and D. K. Sinclair, Phys. Rev. D **70**, 094501 (2004).

[72] M. D'Elia, S. Mukherjee and F. Sanfilippo, Phys. Rev. D **82**, 051501 (2010).

[73] A. J. Mizher, and E. S. Fraga, Nucl. Phys. A **820**, 247c (2009); Nucl. Phys. A **831**, 91 (2009).

[74] A. Barducci, R. Casalbuoni, G. Pettini, and R. Gatto, Phys. Lett. B **301**, 95 (1993).

[75] A. Barducci, R. Casalbuoni, S. De Curtis, R. Gatto, and G. Pettini, Phys. Lett. B **231**, 463 (1989); A. Barducci, R. Casalbuoni, G. Pettini, and R. Gatto, Phys. Rev. D **49**, 426 (1994);